Supplementary Data

S1. NDBF-cysteamine

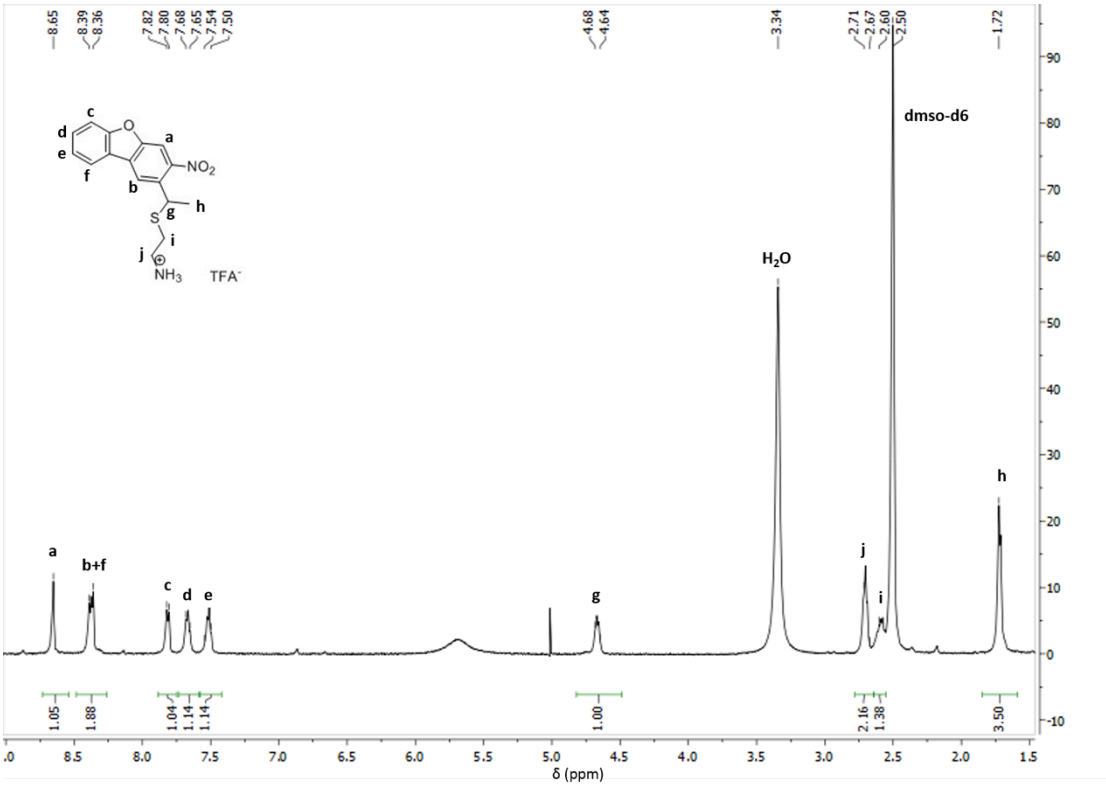

Figure S1. ^{1}H NMR spectrum in DMSO-d_6 (500 MHz) of NDBF-cysteamine.

S2. HA-Furan-NDBF

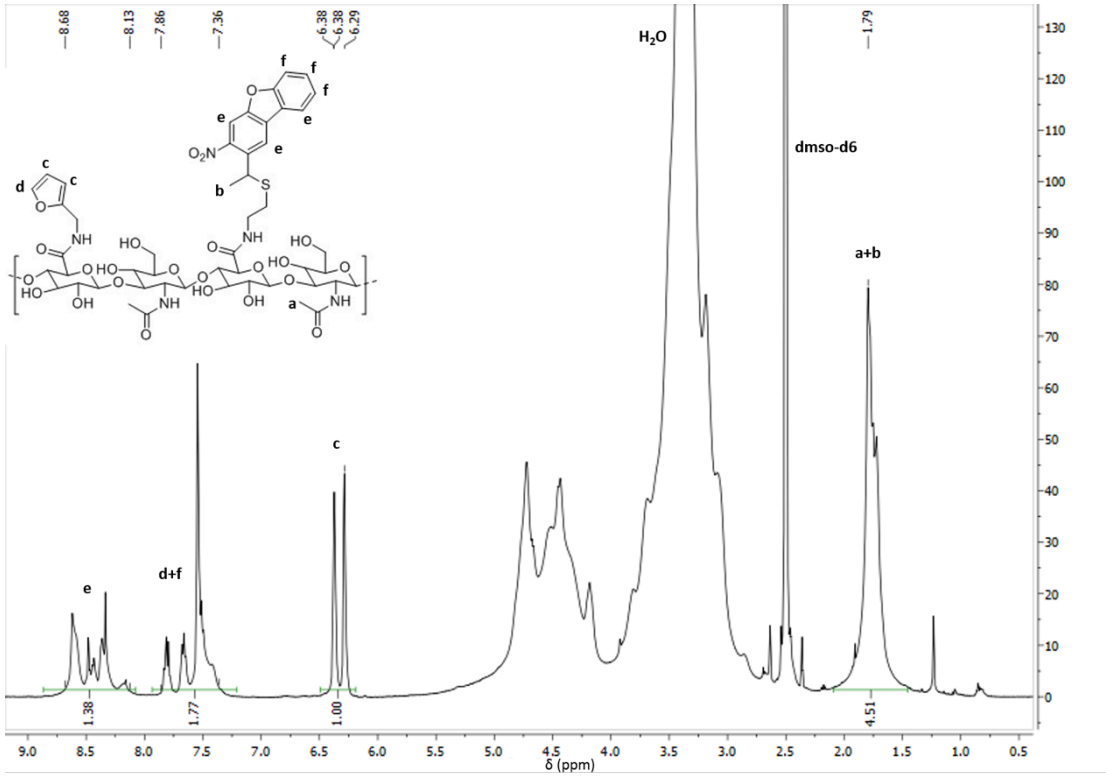

Figure S2. ^{1}H NMR spectrum in DMSO-d_6 (500 MHz) of HA_{NDBF}.

S3. MMPx Sequence and HA-Furan-NDBF Structure

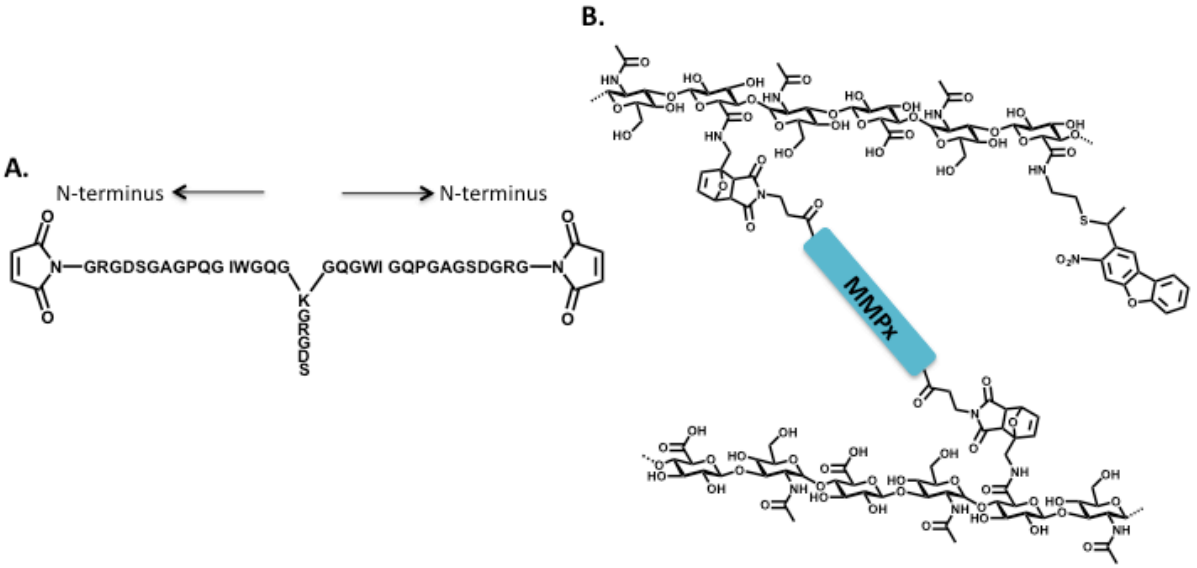

Figure S3. A) The bis-maleimide, MMP cleavable crosslinker, containing three adhesive (GRGDS) sequences and two MMP cleavable sequences (GPQG↓IWGQ). B) Structure of the crosslinked HA_{NDBF}/MMPx hydrogel. HA is modified with furan and NDBF. The bis-maleimide, MMPx peptide reacts with the furan functionalities in a Diels Alder click reaction, forming a crosslinked hydrogel.

S4. Characterization of Biotinylated EGF

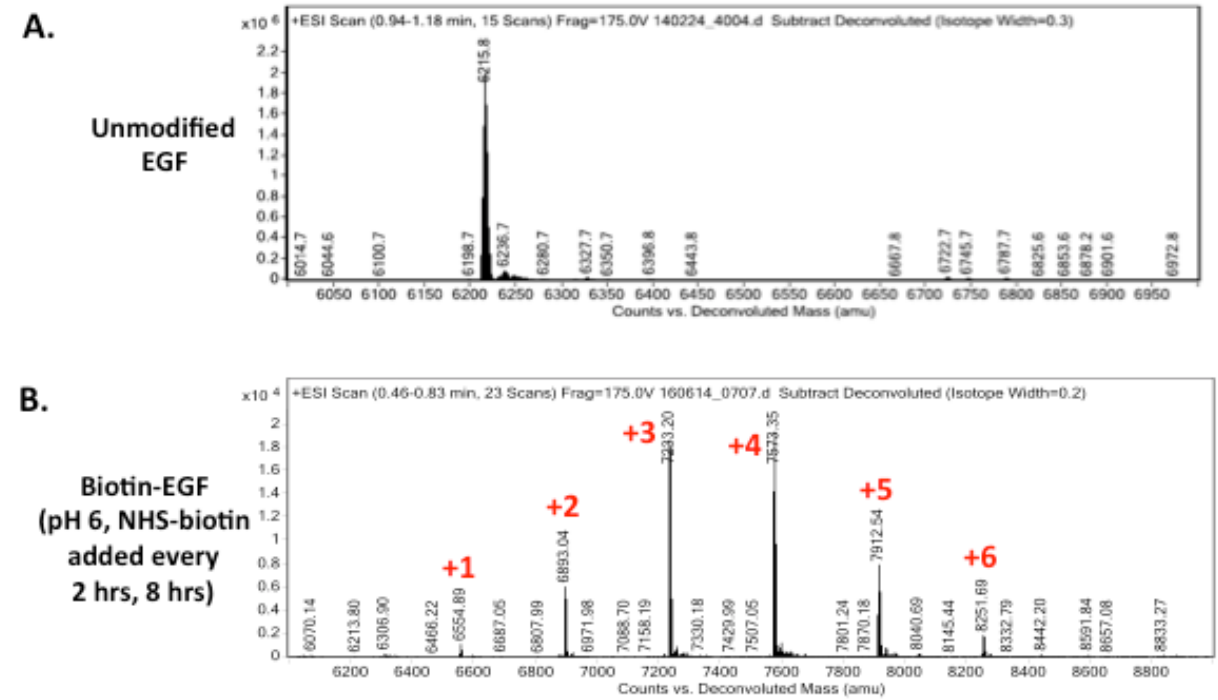

Figure S4. A) Mass spectrum of unmodified EGF (6215.8 amu). B) EGF was modified with biotin by reacting EGF with EZ-Link NHS-LC-biotin in MES buffer (100 mM, pH 6), and then dialyzed against PBS. Mass spectrometry confirmed that EGF had been modified with between 1 and 6 biotin functionalities.

S5. Characterizing Photopatterns in HA_{NDBF} Hydrogels

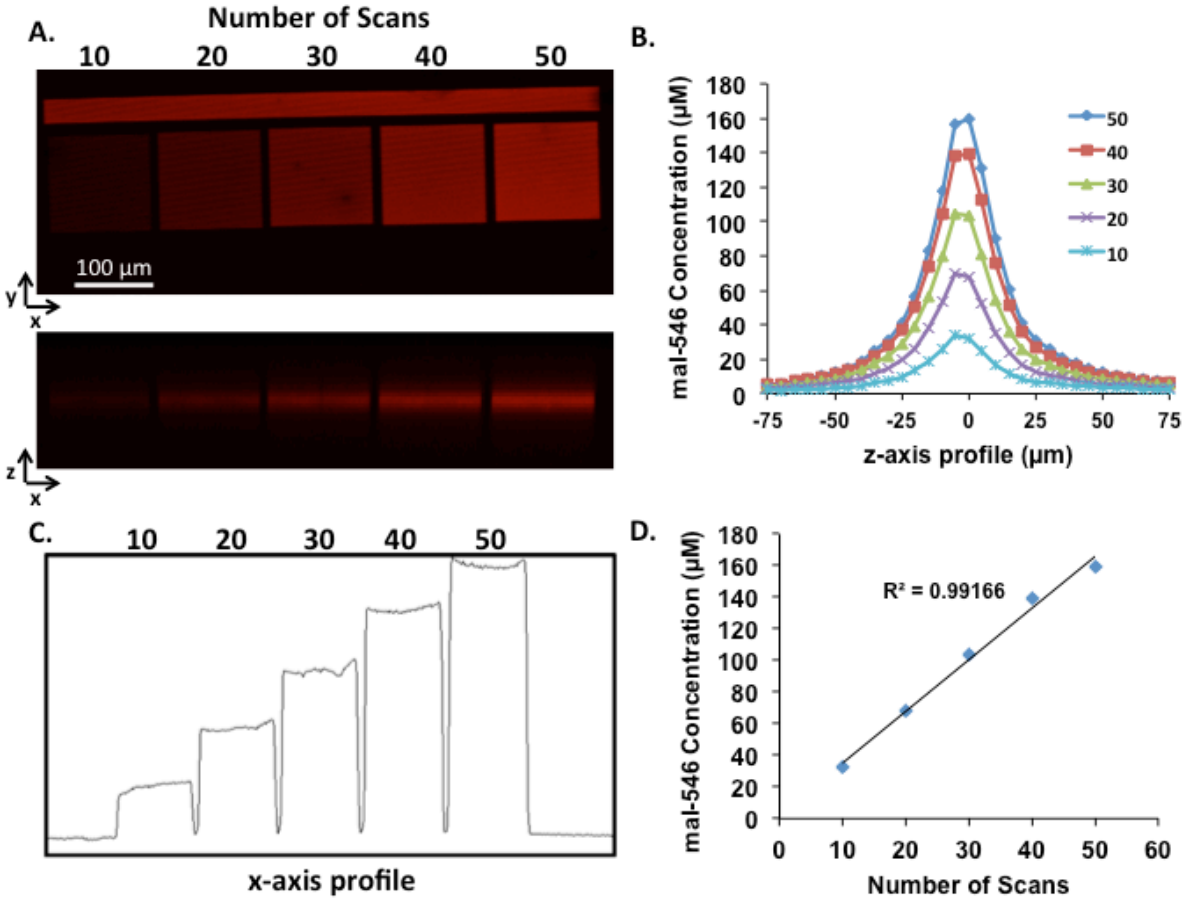

Figure S5. Effect of number of two-photon laser (740 nm) scans on the amount of mal-546 immobilized in HA_{NDBF}/PEG hydrogels. Square x-y planes were patterned at a scan speed of 0.009 µm $µs^{-1}$ and scanned between 10 to 50 times. A) Confocal image depicting square patterns (x-y planes) of immobilized mal-546 in HA_{NDBF}/PEG hydrogels. B) The z-axis profile of the mal-546 square patterns with the maximum intensity is centred at 0 µm. Background mal-546 concentration was subtracted from the immobilized mal-546 concentration. C) The x-axis profile of the mal-546 square patterns. D) The concentration of mal-546 immobilized versus the number of scans.

S6. Photopatterns Can be Created based on ROI

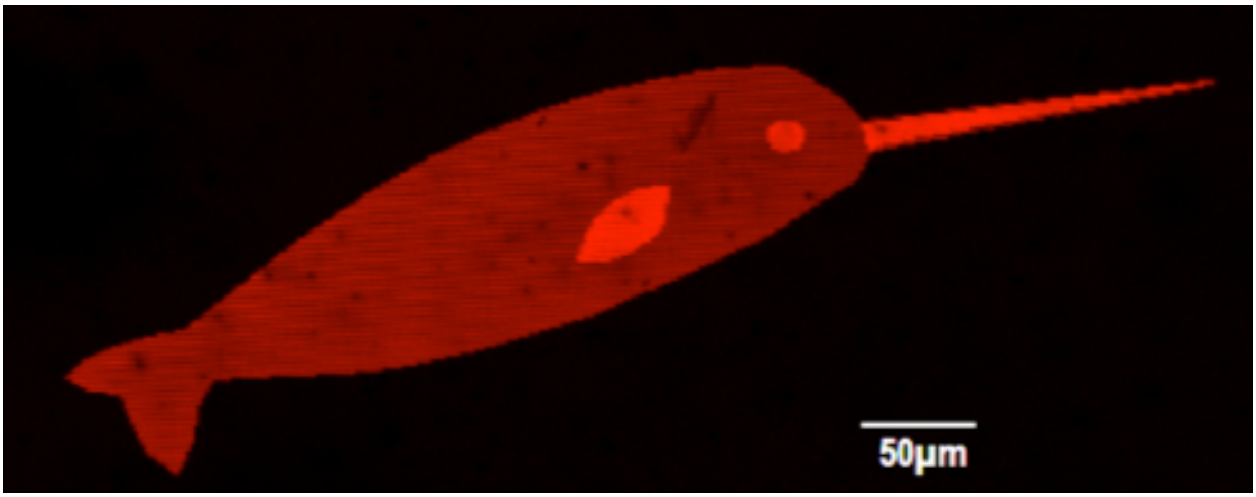

Figure S6. A pattern of a narwhal was formed with mal-546 by scanning an HA_{NDBF}/PEG hydrogel 15 times for the body and 30 times for the fin, tusk and eye at a scan speed of 0.009 µm $µs^{-1}$. This demonstrates the ability to form patterns of many desired shapes.

S7. Bioactivity of EGF555

MCF7 breast cancer cells (7.5 x 10^3 per well) were seeded on 96-well cell culture plates in low serum media (0.5% FBS). Additional media was plated on top of the cells to achieve final EGF or EGF555 concentrations of 0, 10, 20, 50, or 100 ng mL^{-1}. MCF-7 cells were grown for 3 d, fixed with 4% paraformaldehyde and stained with DAPI. Five ROIs were imaged per well and the cell number was quantified using IMARIS Bitplane software.

Both EGF555 and unmodified EGF significantly increased MCF-7 cell number, but there was no significant difference between EGF555 and EGF, as shown in Figure S7.

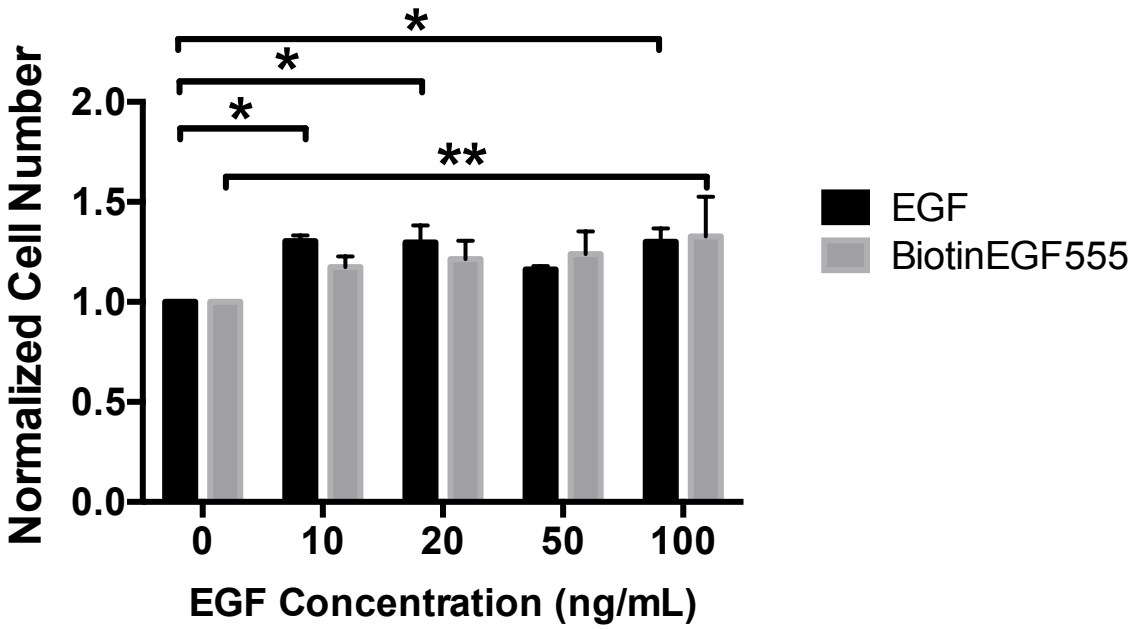

Figure S7. Bioactivity of unmodified EGF and EGF55. Cell number of MCF-7 cells treated with 0, 10, 20, 50 or 100 ng/mL of either EGF or EGF555 for 3 days (n=3, mean + standard deviation). Using a two-way ANOVA, the concentration of EGF was found to significantly influence cell number (****$p<0.0001$). Through post hoc comparisons, MCF-7 cell number was found to be significantly greater at 10, 20, and 100 ng mL^{-1} of EGF compared to the control (0 ng mL^{-1} of EGF, *$p<0.05$). Additionally, MCF-7 cell number was significantly greater with 100 ng mL^{-1} of EGF555 compared to the control (0 ng mL^{-1} of EGF555, **$p<0.01$). At individual EGF concentrations tested, there was no significant difference between EGF and EGF555.

S8. Mechanical Compression Testing

The Young's moduli of the HA hydrogels were measured using 75 µL cylindrical samples formed in chamber well slides with an area of 0.9 cm^2. Following gelation, the hydrogels were quenched with 30 mM N-(2-hydroxyethyl)maleimide in MES buffer (100 mM, pH 5.5) for 24 h at room temperature, washed with PBS (pH 6.8), and then equilibrated in PBS (pH 6.8) containing 50 µM N-(2-hydroxyethyl)maleimide to mimic the maleimide containing molecules present during photopatterning. The hydrogels were irradiated with UV light for 0, 2, 5, 10, or 15 min and placed between two impermeable platens connected to a 150 g force transducer attached to a Mach-1 micromechanical system (Biomomentum). An initial force of 0.075 g force was applied to the hydrogel samples, and the platen-to-platen separation was taken as the initial sample height. The hydrogel disks were compressed to 10% strain with a strain deformation rate of 2% s^{-1}. The strain was then held constant at 10%, while the force was recorded for 60 s. The hydrogels were then compressed in 5 cycles of 2% strain/cycle at a strain deformation rate of 0.4% s^{-1}, with strain held constant for 60 s between each compression cycle. The resultant stress-strain curves of these 5 cycles were averaged to give the Young's modulus of each sample as shown in Figure S8.

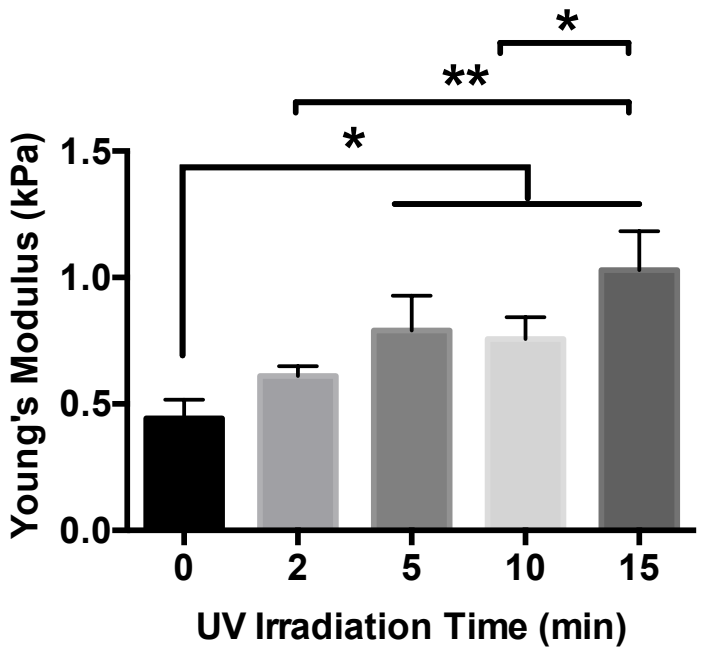

Figure S8. Young's moduli of HA_{NDBF}/MMPx hydrogels irradiated with UV light for 0, 2, 5, 10, or 15 min. Using a one-way ANOVA, irradiation time was found to significantly increase Young's modulus (****$p<0.0001$), with post hoc comparisons displayed graphically ($n>3$, mean + standard deviation). Young's moduli of HA_{NDBF}/MMPx hydrogels irradiated for 5, 10, or 15 min were at least *$p<0.05$ significantly different than hydrogels not irradiated (0 min).

Although we have yet to elucidate the mechanism of the hydrogel stiffening with irradiation, this stiffening only occurred when NDBF was covalently bound to the HA backbone; free NDBF added to the hydrogel did not stiffen the hydrogel with irradiation. Furthermore, the addition of dithiothreitol (to prevent disulphide bond formation between liberated thiols), exogenous furan or maleimide, quenching residual furans with N-(2-hydroxyethyl)maleimide, or hydrolyzing residual maleimides all failed to prevent hydrogel stiffening with irradiation.

This hydrogel stiffening with irradation was not observed in HA hydrogels modified with Bhc; although it should be noted that the efficiency of Bhc photolysis is lower than that of NDBF. The hydrogel stiffening was also observed with both MMPx and bismaleimide-PEG crosslinkers. Given our observations, we believe that the hydrogel stiffening may be a result of a NDBF reactive intermediate reacting with the hydrogel (the hydrogel backbone or the Diels Alder adduct).

S9. MDA-MB-468 Response to EGF in 2D Culture

MDA-MB-468 cells were seeded (5.0×10^3 per well) on 96-well cell culture plates in low serum media (0.5% FBS). Additional media was plated on top of the cells to achieve final EGF or EGF555 concentrations of 0 or 20 ng mL^{-1}. MDA-MB-468 cells were grown for 5 d, fixed with 4% paraformaldehyde and stained with DAPI. Five ROIs were imaged per well and cell number was quantified using IMARIS Bitplane software.

Unmodified EGF (20 ng mL^{-1}) was found to significantly decrease MDA-MB-468 cell number in 2D culture, as shown in Figure S9.

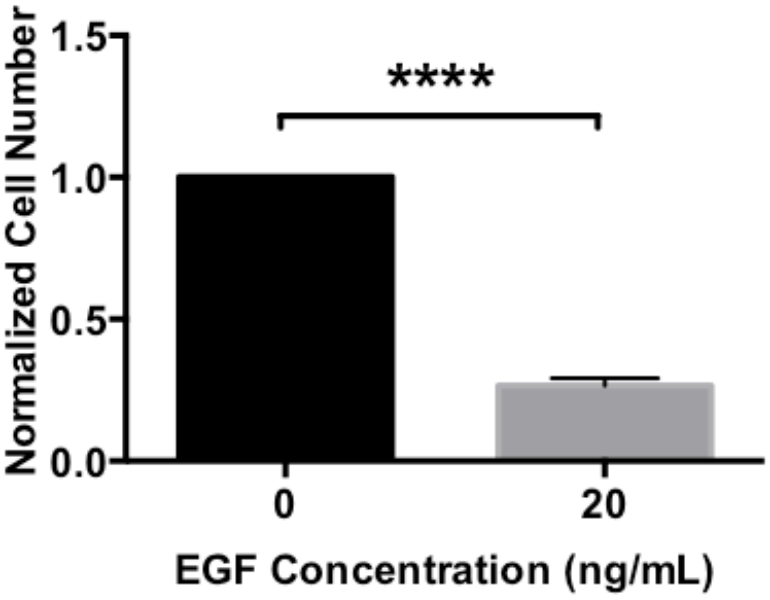

Figure S9. Normalized cell number of MDA-MB-468 cells cultured on 2D with either 0 or 20 ng mL^{-1} of unmodified EGF in the cell culture media. Cell number was quantified after 5 d of culture and normalized to the control (0 ng mL^{-1} EGF), (n=3, mean + standard deviation ****$p<0.0001$). Commercially available, unmodified EGF was found to significantly decrease MDA-MB-468 cell number in 2D culture, supporting the decrease in MDA-MB-468 cell number seen on HA/MMPx hydrogels with EGF555 gradients.